Percolation, sliding, localization and relaxation in glassy circuits

DH and DC
Department of Physics, Ben-Gurion University of the Negev, Beer-Sheva, Israel

There is recent interest in "glassy" systems that have log-wide distribution of relaxation rates [1]. For example we note recent works regarding electron dynamics where the effective model is essentially the same as a *random walk on a disordered lattice* [2, 3]. In such type of model there is a percolation-related crossover to sub-diffusion (in one dimension), or to variable-range-hopping type diffusion (in general) [4]. This crossover is reflected in the spectral properties of the system. A similar point of view regarding percolation is the continuous time random walk (CTRW) with a broad distribution of waiting times [5].

The more general problem of *random walk in random environment*, where transitions between sites are allowed to be asymmetric, has been explored by Sinai [6], Derrida [7], and followers [5, 8]. Focusing on one-dimensional systems, it turns out that for any small amount of disorder an unbiased spreading becomes sub-diffusive. For bias that exceeds a non-zero threshold there is a *sliding transition*, and the drift velocity becomes non-zero. This type of dynamics is relevant to studies in a biophysical context: pulling pinned polymers, DNA denaturation [9, 10], population biology [11, 12], and molecular motors [13, 14]. The bias in the case of depinning polymers and DNA denaturation is the pulling force. In the case of population biology, it is the convective flow of bacteria relative to the nutrients and for molecular motors it is the affinity of the chemical cycle. The sliding transition is a major theme in the latter context.

Considering a finite system, the prototype being an N-site ring, one asks what are the relaxation modes of such a topologically closed system. In the Brownian motor context N is the length of a cycle, i.e. the number of chemical reactions required to advance the motor by one step. In the remaining examples, sites have a spatial context and the number of sites N arises from the underlying lattice.

A complementary question regarding the "delocalization" of eigenstates of non-Hermitian quantum Hamiltonians has been addressed by Hatano, Nelson, and followers [15–17], originally in the context of vortex depinning in type II superconductors. In this case, the bias is the applied transverse magnetic field and N is the number of defects to which the magnetic vortex can pin. Their main achievement is the realization that the complex spectrum of the non-Hermitian hamiltonian can be deduced from the real spectrum of an associated Hermitian hamiltonian. Various improvements on the method and ensuing analytical results were obtained. For example, the complex spectrum in the thermodynamic limit was found in [18]. An equation for the curve in the complex plane on which the eigenvalues are located and the density of states was found in [19]. Results for special models of one impurity and one way dynamics (maximally asymmetric transition rates) were obtained in [20].

We show below that for a conservative "random walk" dynamics the implied spectral properties are dramatically different. Notable "conservative random walkers" are Brownian motors. For example, molecular motors on heterogeneous tracks, such as DNA or RNA. In [13, 14] non conservative motors are considered. It was found that under an external force and strong disorder, the motor will become localized at preferred positions yet near the stall force, localization occurs for any amount of disorder. These results were obtained by observing the numerically obtained spectrum.

I. STOCHASTIC SPREADING

Diffusive spreading.– Einstein has considered in his thesis the problem of Brownian motion. This can be regarded as a stochastic process in which a particle hops from site to site with some hopping rate w. The rate equation can be written in matrix notation as

$$\frac{d\boldsymbol{p}}{dt} \;=\; \boldsymbol{W}\boldsymbol{p}, \tag{1}$$

involving a matrix $\boldsymbol{W}$ whose off-diagonal elements are the transitions rates w_{nm}, and with diagonal elements $-\gamma_n$ such that each column sums to zero. For example, in the case of a one-dimensional lattice with near-neighbor hopping

$$\boldsymbol{W} \;=\; \begin{bmatrix} -\gamma_1 & w_{1,2} & 0 & ... \\ w_{2,1} & -\gamma_2 & w_{2,3} & ... \\ 0 & w_{3,2} & -\gamma_3 & ... \\ ... & ... & ... & ... \end{bmatrix} \tag{2}$$

with $\gamma_n = \sum_{m(\neq n)} w_{mn}$. Einstein's theory assumes a symmetric matrix $\boldsymbol{W}$. The diffusion coefficient is $D \sim wa^2$, where w is the average hopping rate between neighboring sites, and a is the average distance between them. The associated negative eigenvalues $\{-\epsilon_k\}$ of the matrix $\boldsymbol{W}$ are characterized by the spectral density

$$\rho(\epsilon) = \text{const}\ \epsilon^{\mu-1} \quad \text{(for small } \epsilon\text{)} \tag{3}$$

where $\mu = d/2$, and $d = 1,2,3$ is the dimensionality. It is physically appealing to think of $\boldsymbol{W}$ as the Hamiltonian matrix of a particle on a lattice, and then $-\epsilon_k$ are the eigen-energies. Optionally the w_{nm} may represent spring-constants, and then $\omega_k = \sqrt{\epsilon_k}$ are the Debye frequencies of the vibrational modes.

Percolation transition.– The first question that arises is how is Einstein's result affected if the rates come from some wide distribution. The simplest model assumes randomly distributed sites, and rates that depend exponentially on the distance $w \propto \exp(-r/\xi)$. For such a type of model the distribution of the rates is

$$P(w) = \text{const}\ w^{\alpha-1} \quad \text{(for small } w\text{)} \tag{4}$$

where $\alpha = \xi/a$ and a is the mean spacing. If the distance between the sites is increased, α decreases. As the network becomes "glassy" ($\alpha < 1$) there is a percolation-related transition to very slow diffusion ("variable range hopping"). This holds for any dimension $d > 1$. For one dimension ($d = 1$) there is a more dramatic transition to sub-diffusion. In the later case the spectral density is no longer $\mu = d/2 = 1/2$, but ([21])

$$\mu[\text{of symmetric matrix}] \;\; = \min\left\{\frac{\alpha}{1+\alpha} \;\;,\;\; 1/2\right\} \qquad (5)$$

Sinai spreading.– The second question that arises is what happens to Einstein's theory if the transition rates are asymmetric. This question has been addressed by Sinai, Derrida and followers [6, 7], sometimes called "random walk in random environment". We define the stochastic field as

$$\mathscr{E}_{m\rightsquigarrow n} \;\; \equiv \;\; \ln\left(\frac{w_{nm}}{w_{mn}}\right), \qquad (n \neq m) \qquad (6)$$

such that the ratio of "backward" to "forward" transitions equals a Boltzmann factor $\mathrm{e}^{-\mathscr{E}}$. For the purpose of presentation we assume that the stochastic field has box distribution within $[s-\sigma, s+\sigma]$. The average value s, the so called affinity, determines the direction of the drift velocity $v = v_\sigma(s)$. It is well known that by a similarity transformation the $\boldsymbol{W}$ of an *open* chain becomes a symmetric matrix $\boldsymbol{H}$. The associated spectrum $\{-\epsilon_k\}$ consists of real negative values, and is characterized by a spectral density $\rho(\epsilon)$ that is discussed below.

Sliding transition.– Consider a sample of N sites. For $s \ll 1/N$ the Einstein relation implies that $v/D = s$. For larger s the ratio becomes smaller, and eventually for a very large s it saturates $v/D \to 2/a_\sigma$. The length scale a_σ depends on the disorder σ, and equals the lattice constant in the absence of disorder ($a_0 \equiv 1$). In the limit $N \to \infty$ it has been established that $v_\sigma(s) = 0$ up to some critical value s_1. For $s > s_1$ the drift velocity becomes finite, which we call "sliding transition". The s dependence of the diffusion coefficient $D = D_\sigma(s)$ is more complicated: it is vanishingly small up to some value $s_{1/2}$, then it becomes infinitely large up to some critical value s_2, while for larger s it becomes finite. The sliding-transition threshold s_μ is determined solely by the μth moment of $\mathrm{e}^{-\mathscr{E}}$, and is not affected by the $P(w)$ distribution (see appendix (B)). By inverting the relation $s = s_\mu$ we get the exponent that characterizes the spectral density $\rho(\epsilon)$, namely

$$\mu[\text{of asymmetric matrix}] \;\; = \;\; \mu_\sigma(s) \;\; \in \;\; [0,\infty] \qquad (7)$$

This implies that the spreading process is anomalous. By definition for $s > s_\infty$ we get $\mu = \infty$, meaning that a gap is opened: the lowest eigenvalue has a non-zero N-independent finite value. For zero disorder $\epsilon_0 = v^2/(4D) \propto s^2$ is the characteristic rate of drift limited relaxation. For the assumed box distribution $s_\infty = \sigma$, so for very large disorder $\epsilon_0 \propto \exp[(s-\sigma)/2]$ is the minimal transition rate of the network.

Relaxation.– We close an N-site chain into a ring. Now a topological aspect is added to the problem, and one wonders what are the relaxation modes of the system. It should be clear that in a closed system the lowest eigenvalue is always $\lambda_0 = 0$, while all the other eigenvalues $\{-\lambda_k\}$ have negative real part, and may have an imaginary part as well. Complex eigenvalues imply that the relaxation is not over-damped: one would be able to observe an oscillating density during relaxation, as demonstrated in Fig. 1. The work of [17], regarding the dynamics that is generated by non-Hermitian quantum Hamiltonians, has considered what happens to the spectrum of a non-conservative matrix $\boldsymbol{W}$ whose diagonal elements γ_n are *fixed*. As s (as defined after equation (6)) is increased beyond a threshold value s_c, the eigenvalues in the middle of the spectrum become complex. As s is further increased beyond some higher threshold value, the entire spectrum becomes complex. However, we see that this is not the case in our system: **(a)** The delocalization starts at the bottom of the band (see second row of Fig. 3 for examples of the spectrum in the complex plane); **(b)** Asymptotically only a finite fraction of the spectrum becomes complex. We name the latter effect *saturation of complexity*, this is demonstrated in Fig. 7.

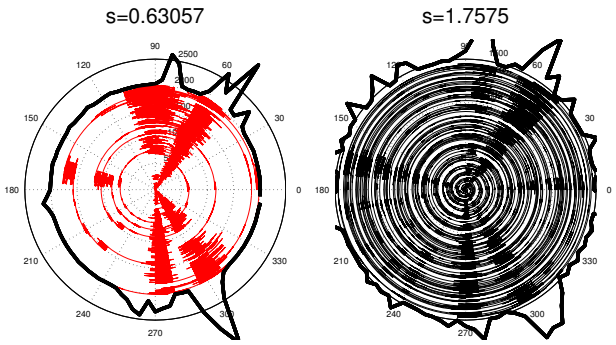

FIG. 1. Simulated trajectory of a particle on a disordered ring. For small s (left panel) the dynamics is overdamped, while for large s (right panel) the dynamics is under damped. The radial direction is time. The thick line on the edge of the circle is the steady state distribution. For this figure there are $N = 100$ sites and $\sigma = 3$.

II. SCOPE

Our objective is to understand how the spectral properties of the $\boldsymbol{W}$ matrix are affected as the affinity s is increased. A crucial observation is that the conservative property of the matrix implies that s affects not only the stochastic field, but also the diagonal elements. As in the work of [17] we can transform $\boldsymbol{W}$ into a non-hermitian $\boldsymbol{H}$ matrix. This matrix features the following properties: **(i)** Off-diagonal disorder characterized by α; **(ii)** An affinity parameter s. **(iii)** Diagonal disorder that is implied by the conservativity. It is the last property that implies a dramatically different spectral scenario. In particular we would like to address the following questions: **(1)** How does the relaxation rate of the system depend on s? **(2)** What determines the threshold s_c for getting a complex quasi-continuum? **(3)** Why is there, and what determines the saturation of complexity? **(4)** How is the sliding transition reflected in the spectrum? **(5)** How is the percolation transition reflected in the spectrum?

In order to answer the above questions we translate the spectral problem into the language of Electrostatics in the two dimensional complex plane. **(a)** We first explain that in the absence of field disorder ($\sigma = 0$) the delocalization process is determined by the percolation transition. We argue that for $\alpha < 1/2$ the system is localized for any s and that for $\alpha > 1/2$ the system becomes delocalized for any $s > 0$. **(b)** We address the simplest problem of a clean N-site ring with sparse field disorder. We explain that $s_c \sim \sigma\sqrt{M}/N$, which is the field required to overcome M field defects. **(c)** Then we discuss a fully disordered ring. We show how the sliding transition thresholds s_μ are expressed in the spectral properties. In particular we show that $s_c \to s_{1/2}$, which is the field required to get a sliding transition for D. **(d)** For $s > s_\infty$ the real spectrum of an open chain is gapped. But for a closed ring the delocalization transition leads to a non-gapped complex λ-spectrum, that exhibits complexity saturation. We explain how the percolation-related transition affects the delocalization process. **(e)** Complexity saturation...

III. OUTLINE

- The secular equation for λ_k
- The real spectrum ϵ_k (discussing μ_s and μ_α)
- The complex spectrum - Electrostatics
- Determination of s_c
- Complexity diminishes the real gap
- Complexity saturation for $s \gg s_\infty$

Supplementary

- Sliding transition - the definition of s_μ.
- The similarity transformation (definition of H)
- The formula for the spectral determinant.
- Clean ring
- Ring with weak link ("g")
- Ring with single field defect
- Ring with white disorder ("French")
- Step by step electrostatics

IV. THE SECULAR EQUATION

Consider a stochastic process on an N-site ring with lattice spacing $a = 1$, that is generated by a rate equation with near-neighbor hopping as described by the matrix $\boldsymbol{W}$ of equation (2), where the site index n is defined modulo N. For convenience we use the following notations:

$$\overrightarrow{w}_n = w_{n+1,n} \;=\; w_n\, \mathrm{e}^{+\mathscr{E}_n/2} \tag{8}$$

$$\overleftarrow{w}_n = w_{n,n+1} \;=\; w_n\, \mathrm{e}^{-\mathscr{E}_n/2} \tag{9}$$

The question arises whether the sliding transition affects the global properties of the spectrum. In order to address this question we have to analyze the secular equation that is associated with the matrix $\boldsymbol{W}$.

By a similarity transformation of $\boldsymbol{W}$ one obtains

$$\tilde{\boldsymbol{W}} \;=\; \mathrm{diagonal}\{-\gamma_n\} \;+\; \mathrm{offdiagonal}\{w_n \mathrm{e}^{\pm s/2}\} \tag{10}$$

where the "$\pm$" are for the "forward" and "backward" transitions respectively. Note that the statistics of the $\mathscr{E}_n$ is still hiding in the diagonal elements. The associated symmetric matrix $\boldsymbol{H}$ is defined by setting $s = 0$. Then one can define a spectral determinant $S(z)$ and associated spectrum as follows:

$$\det(z - H) \;=\; \prod_k (z + \epsilon_k) \;=\; S(z) \tag{11}$$

If the system is an N-periodic infinite lattice, then $\boldsymbol{W}$ is similar to $\boldsymbol{H}$ by "gauge" transformation, hence one can regard the $\{-\epsilon_k\}$ as the spectrum of an open chain. But if the system is an N-periodic ring (periodic boundary conditions) then s cannot be "gauged" away. Still there is a simple relation [23] that relates the spectral determinant of $\boldsymbol{W}$ to that of $\boldsymbol{H}$. Namely,

$$\det(z - W) \;=\; \prod_k (z + \lambda_k) \;\equiv\; S(z) - S_0 \tag{12}$$

where

$$S_0 \;=\; 2\left[\cosh\left(\frac{Ns}{2}\right) - 1\right] \prod_n w_n \tag{13}$$

The roots $z = -\lambda_k$ have real negative part, but may be complex in general. The lowest eigenvalue $\lambda_0 = 0$ corresponds to the non-decaying non-equilibrium steady state (NESS). It is implied that

$$S(0) = S_0 \qquad \text{implication of conservativity} \tag{14}$$

We emphasize that the latter property is not true for a general non-Hermitian matrix, neither is the "positivity" of the λ_k. This has far reaching implications: in particular it should be clear that the NESS is an extended state, hence it follows that the localization length has to diverge in the limit $\lambda \to 0$. This is in essence the difference between the conventional Anderson model (Lifshitz tails at the band floor) and the Debye model (phonons at the band floor).

From the above it follows that the secular equation for the λ spectrum can be written as

$$\prod_k \left(\frac{z + \epsilon_k(s)}{\overline{w}}\right) \;=\; 2\left[\cosh\left(\frac{Ns}{2}\right) - 1\right] \tag{15}$$

where $\overline{w}$ is the geometric average of all the rates. The affinity s affects both the ϵ_k and the right hand side.

V. THE REAL SPECTRUM

The main observation regarding the real spectrum ϵ_k of the associated symmetric matrix $\boldsymbol{H}$ is that for $s < s_\infty$ it is gapless and for $s > s_\infty$ a gap opens up. This can be seen both in the spetcral density and in the electrostatic potential along the real

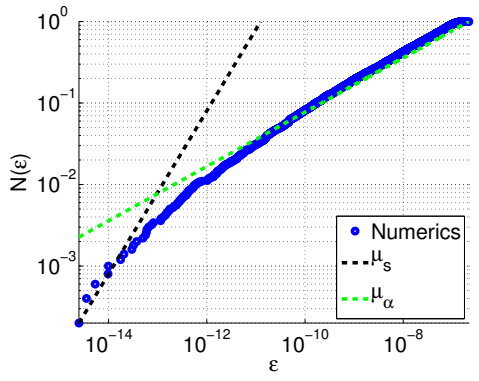

FIG. 2. The integrated density of the ϵ_k for a ring with $N = 5000$ sites. The system is characterized by a percolation exponent $\mu_\alpha = 1/3$ and a scaled affinity $\mu_s = 1$. The width of the stochastic-field distribution is $\sigma = 2$. The blue points are are results of numerical diagonalization. There is a crossover from density that corresponds to μ_s (dashed black line) to density that corresponds to μ_α (dashed green line).

axis. Recall that $\rho(\epsilon) \sim \epsilon^{\mu-1}$. Consider first the case $\alpha \gg 1$, the percolation aspect is absent and $\mu = \mu_s$. The simplest case is for $s > s_\infty$, where a gap opens up at $\epsilon_0 = e^{(s-\sigma)/2}$ and the spectral density is distributed log-box, $\rho(\epsilon) = N/\sigma\epsilon$. This holds as long as $\alpha \gg 1$. The interesting case is when $\alpha \lesssim 1$ and $s < s_\infty$, now there is a crossover in the spectrum between two anomalous behaviours. The bottom of the band is detemined by μ_s and the top of the band by μ_α, as show in Fig.2. As α decreases, the μ_s determined region becomes smaller. This crossover is analogous to regular diffusion, where there is a crossover from short time, diffusion limited spreading to long time drift limited spreading. In our case the crossover is from low energy (long time) sliding (μ_s) to high energy (short time) percolation limited diffusion μ_α.

We remark that the the case of a continuous and open system with stochastic field that is guassian white noise has been studied extensively in [8]. Exact analytical results for the density of states and inverse localization (electrostatic potential) length were obtained (these are summarized in appendix (I)). The electrostatic potential is quite different, it has a peculiar trait that $V(\epsilon \to \infty) = \text{const}$, implying that the entire spectrum goes from real to complex at $s = s_{1/2}$.

VI. ELECTROSTATICS

In order to get an insight into the secular equation we define an "electrostatic" potential as follows:

$$\Psi(z) \;=\; \sum_k \ln\left(\frac{z-\epsilon_k}{\overline{w}}\right) \;\equiv\; V(x,y) + iA(x,y) \qquad (16)$$

where $z = x + iy$. Note that compared with equation (10) we have flipped the sign convention ($z \mapsto -z$). The potential for a given charge distribution $\rho(x)$ is

$$V(x,y) = \frac{1}{2}\int \ln\left[(x-x')^2 + y^2\right]\rho(x')dx' \qquad (17)$$

and along the real axis it is

$$V(\epsilon) = \int \ln\left(|\epsilon - x|\right)\rho(x)dx \qquad (18)$$

The constant $V(x,y)$ curves correspond to potential contours, along which $|S(z)|$ is constant, and the constant $A(x,y)$ curves corresponds to stream lines, along which the phase of $S(z)$ is constant. The derivative $\Psi'(z)$ corresponds to the field, which can be regarded as either electric or magnetic field up to a 90deg rotation. Using this language the secular equation takes the form

$$V(x,y) = V(0); \quad A(x,y) = 2\pi * \text{integer} \qquad (19)$$

Namely the roots are the intersection of the field lines with the potential contour that goes through the origin.

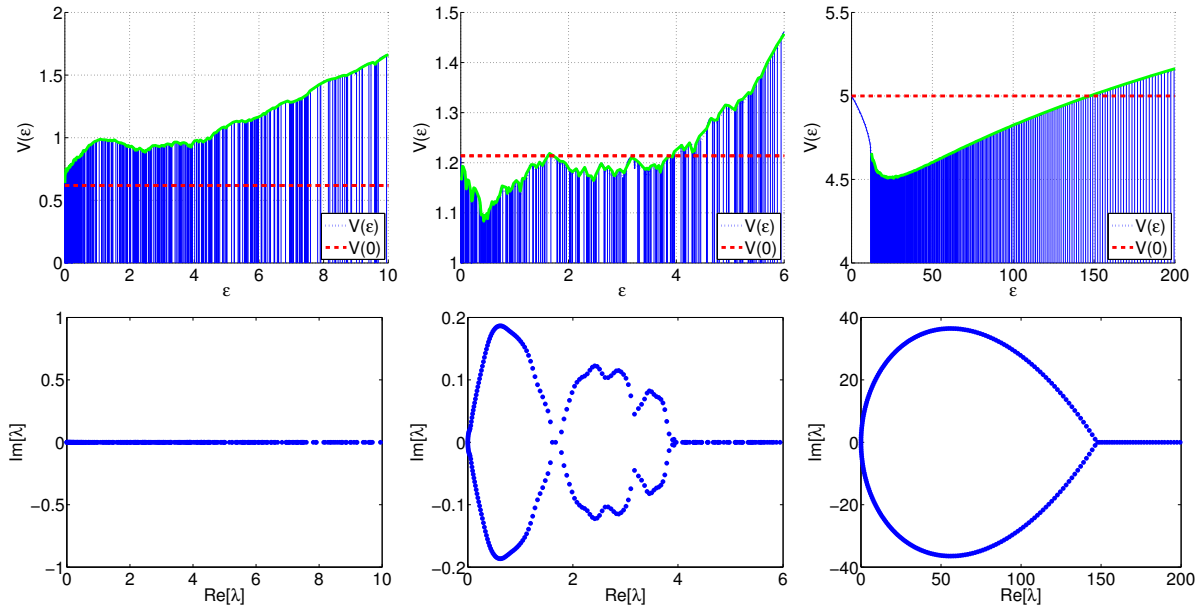

FIG. 3. Illustrating the route to complexity. The top row shows the electrostatic potential $V(\epsilon)$ along the real axis and the bottom row shows the associated spectrum in the complex plane. Here $N = 500$, $\sigma = 5$, and (from left to right) $s = 1.24,\ 2.43,\ 10$. For these parameters the threshold values are $s_{1/2} = 1.77,\ s_1 = 2.7$ and $s_\infty = 5$. In the left hand column $s < s_{1/2}$ and the spectrum is real. In the middle column $s_{1/2} < s < s_\infty$ and there is an interesting scenario of a mixed spectrum, where there might be several complex bubbles separated by real segments. In the right hand column $s > s_\infty$ and the real spectrum has a gap (beginning with the first oscillation), but the complex spectrum does not (see also Fig.6). Also, the spectrum is a fully developed complex bubble, where the bottom of the band is delocalized (underdamped modes) and the rest of the band is localized (or overdamped).

VII. DETERMINATION OF s_c

From the preceding section we know that the potential at the origin is

$$V(0) \;=\; \ln\left[2\cosh\left(\frac{Ns}{2}\right)-2\right] \tag{20}$$

From a straightforward electrostatic calculation we find that for a charge density that is given by equation (3) with some cutoff ϵ_c, the derivative of the electrostatic potential at the origin is given by (see appendix (A) for derivation)

$$V'(\epsilon) \approx \frac{\epsilon^{\mu-1}}{\epsilon_c^{\mu}}\pi\mu\cot(\pi\mu) \tag{21}$$

Indicating that the sign changes from positive to negative at $\mu = 1/2$.

Let us make a few observations regarding the potential $V(\epsilon)$ along the real axis. For an illustration see Fig.3. Clearly if the envelope of $V(\epsilon)$ is above the $V = V(0)$ line, then the spectrum is real, and the λ_k are roughly the same as the ϵ_k, shifted a bit to the left. The second observation is that the envelope of $V(\epsilon)$ is positive in segments where the ϵ_k forms a quasi-continuum. This follows from the observation that $(1/N)V(\epsilon)$ equals the inverse localization length [17]. In the case under study the quasi-continuum starts at $\epsilon_s = 0$ for $s < s_\infty$ (Fig.3), and at finite ϵ_s for $s > s_\infty$ (Fig.6). If follows that the threshold s_c f,or getting a complex quasi-continuum is either $V'(0) < 0$ or $V(\epsilon_s) < V(0)$ respectively. In the former case it follows from equation (21) that $s_c = s_{1/2}$.

A. Determination of s_c - Random resistor network with uniform field

We consider now the case where all of the bonds are random and the field is uniform, $s \neq 0,\ \sigma = 0$. Using the electrostatic picture we have shown that $\mu = 1/2$ provides the threshold value for complex eigenvalues. All one has to do is determine what is μ for the problem at hand. Recall that μ is the exponent of the associated real spectrum of $\boldsymbol{H}$. For $s = 0$, we already know μ is given by equation (5). For large s, the matrix $\boldsymbol{H}$ is characterized by very large diagonal elements, $\gamma_k = w_k e^{s/2} \gg w_k$ and is thus "trivially localized" with eigenvalues $\epsilon_k = \gamma_k$. Therefore $\mu(s \gg 1) = \alpha$, by definition of w_k (equation (4)), while for small s, the exponent is given by equation (5). So, for $\alpha < 1/2$ also $\mu < 1/2$ and the electrostatic picture tells us that the spectrum must be real, regardless of s. On the other hand, if $\alpha > 1/2$ also $\mu > 1/2$ and the spectrum will become complex for any finite $s > 0$.

B. Determination of s_c - white vs. sparse field disorder

The simplest case to exhibit a crossover to a complex spectrum is that of a single defect. There are two types of defects, either in the couplings w_n or in the fields $\mathscr{E}_n$. The details are slightly different, but the analysis is essentially the same. The spectrum ϵ_k of the symmetric matrix $\boldsymbol{H}$ has two components: A continuum in the range $2\cosh(s/2)\pm 2$ and two additional states. There are two additional states because by changing a single bond, two decay rates are altered. In the language of electrostatics we have a continuous charge distribution and two point charges γ_1,γ_2. In general, one of these charges is immersed in the continuum and one of the charges is isolated, either well above or well below the continuum. Since the continuum does not contribute to the potential $V(\epsilon_s)$ (see appendix (J)), in the end

$$V(\epsilon_s) = V(|\gamma_i - \epsilon_s|) \tag{22}$$

where $V(|\gamma_i-\epsilon_s|)\approx \ln\gamma_i$ is the potential at ϵ_s, generated by a single charge at a distance $|\gamma_i-\epsilon_s|$ from the continuum. All that is required now it to find the γ_i's for the configuration at hand.

For a single defect in the stochastic field the decay rates are

$$\gamma_0 = 2\cosh(s/2) \tag{23}$$
$$\gamma_1 = e^{(s+\sigma)/2} + e^{-s/2} \tag{24}$$
$$\gamma_2 = e^{-(s+\sigma)/2} + e^{s/2} \tag{25}$$

where γ_1 is above the continuum and γ_2 is immersed in the continuum, thus $V(\epsilon_s)=\ln\gamma_1\approx\sigma/2$, so from the condition that $V(\epsilon_s)=V(0)$ we get

$$s_c = \sigma/N \tag{26}$$

Note that this result can be obtained in the continuum limit (see Appendix).

This argument can be extended to the case of M defects, under the assumptions that the field strength of each defect is different and that the defects are well separated. If there are M field defects of varying strength $\sigma_i\in[-\sigma,\sigma]$ then there are M isolated charges $\gamma_i\approx e^{\sigma_i/2}$, so the potential is

$$V(\epsilon_s) = \sum_{i=1}^{M}\ln\gamma_i = \frac{1}{2}\sum_{i=1}^{M}\sigma_i \sim \frac{\sigma\sqrt{M}}{2} \tag{27}$$

From the condition $V(\epsilon_s)=V(0)$, one gets the threshold value

$$s_c = \frac{\sigma}{N}\sqrt{M} \tag{28}$$

Of course this approximation breaks down at some finite value of defect density M/N since the assumption that the defects are well separated is no longer valid. At this point there should be a crossover to the fully disordered behaviour where $s_c\to s_{1/2}$. In the numerics this happened at $M/N\sim 0.1$. This sparse disorder approximation is tested in Fig.4.

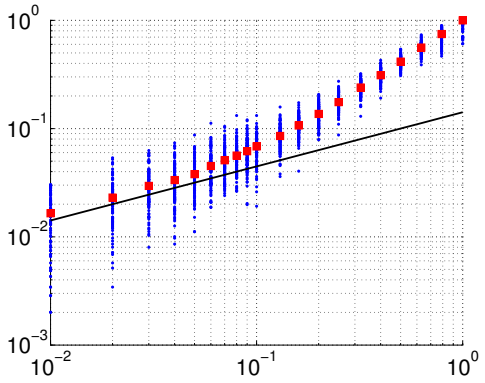

FIG. 4. The threshold value s_c for the spectrum to be complex vs. the number of stochastic field defects M. Here $N=100$ sites and $\sigma=5$. The x axis is the fraction of the lattice that has a disordered field, the rest of the lattice has a uniform field. For a fully disordered lattice we expect $s_c=s_{1/2}$, hence the scaling of the y axis. The black line is the sparse disorder approximation, equation (28). Blue dots correspond to 100 different realizations of disorder per M/N, red dots are their averages.

C. Determination of s_c - weak link

Consider now a single defect in the couplings, such that $w_1=g$, $w_{n\neq 1}=1$ where $g\ll 1$. This setup can be treated exactly in the continuum limit, yet we can use the electrostatic picture to obtain an estimate for s_c in the discrete lattice. In the continuum limit one considers a ring of length L with diffusion coefficient D. A small segment of length $a\ll L$ has diffusion coefficient $D_1\ll D$ such that $G=(L/a)(D_1/D)$ is the relative strength of the weak link. By standard transfer matrix methods one can derive the secular equation for the complex eigenvalues (see appendix (G))

$$\cos(k) + \frac{1}{G}\frac{k^2+(\frac{S}{2})^2}{2k}\sin(k) = \cosh\left(\frac{S}{2}\right) \tag{29}$$

where $k^2 = zL^2/D - S^2/4$ is generally complex. The envelope of the secular equation is

$$A(z) = \sqrt{1+\frac{1}{G^2}\frac{z^2}{4z-S^2}} \tag{30}$$

and is related to the electrostatic potential by $\Psi(z)=2A(z)-2$. This function has a minimum at $z=S^2/2$, thus the secular equation has real solutions provided

$$\sqrt{1+\left(\frac{S}{2G}\right)^2} > \cosh\left(\frac{S}{2}\right) \tag{31}$$

For $S/G\gg 1$ this equation becomes approximately $S/2G = e^{S/2}$. The solution is given in terms of the Lambert W function

$$S_c = -2W(-G/2) \tag{32}$$

Returning to the discrete model, we notice that $g=NG$. The spectrum of the associated Hermitian matrix $\boldsymbol{H}$ is composed of a single state ϵ_1, which is the ground state and a

quasi-continuum which begins at $\epsilon_s > \epsilon_1$. The ground state is pushed down from the quasi-continuum. For small S the ground state is approximately (see appendix (G 1))

$$\epsilon_1 \approx \frac{S^2}{4}\frac{g}{1-g} \tag{33}$$

so the potential at ϵ_s is

$$V(\epsilon_s) \approx \ln\left|\frac{\epsilon_s-\epsilon_1}{g}\right| = \ln\left[\frac{s^2}{4}\frac{1-2g}{g(1-g)}\right] \tag{34}$$

where we have neglected the contribution of the continuum to the potential. Clarify the circumstances where this agrees or disagrees with equation (31).

VIII. COMPLEXITY DIMINISHES THE REAL GAP

For a clean ring (no disorder) the stochastic field is uniform ($\mathscr{E} = s$) and all the couplings are the same ($w_n = w$). The drift velocity and the diffusion coefficient are

$$v_0(s) = (\overrightarrow{w} - \overleftarrow{w}) = 2w\,\sinh(s/2) \tag{35}$$

$$D_0(s) = \frac{1}{2}(\overrightarrow{w} + \overleftarrow{w}) = w\,\cosh(s/2) \tag{36}$$

The continuum limit is transparent, and corresponds to the solution of a diffusion equation with a drift term. It is easy to see that the eigenvalues $\{-\lambda_n\}$ of the $\boldsymbol{W}$ matrix are

$$\lambda_n = 2w\left[\cosh\left(\frac{s}{2}\right) - \cos\left(\frac{2\pi}{N}n + i\frac{s}{2}\right)\right] \tag{37}$$

The non-equilibrium steady state (NESS) is associated with $\lambda_0 = 0$. The complexity of the other eigenvalues implies that the relaxation process in not over-damped. Even without any mathematics it is quite clear that the relaxation rate Γ is limited by the lowest diffusion mode, namely

$$\Gamma = \mathrm{Re}[\lambda_1] = \left(\frac{2\pi}{N}\right)^2 D \tag{38}$$

It is also physically clear that if the ring is "opened", or optionally if one of the links is removed, then the relaxation becomes drift-limited. The result is

$$\Gamma = 2w\left[\cosh\left(\frac{s}{2}\right) - 1\right] \sim \frac{v^2}{4D} \tag{39}$$

It is important to realize that in the latter case we have a "gap" in the spectrum, meaning that λ_1 does does not diminish in the $N \to \infty$ limit.

In Fig.5 we calculate $v(s)$ and $D(s)$ for a ring with disorder, deduce from it Γ using equation (38), and compare with the numerically determined $\mathrm{Re}[\lambda_1]$. We deduce that the non-monotonic behaviour of Γ can be explained by the known theory of the sliding transition.

Turning to the disordered ring, we show that even though the real spectrum of $\boldsymbol{H}$ is gapped for $s > s_\infty$ with a quasi continuum beginning at the N-independent value $\epsilon_0 \propto \exp[(s-\sigma)/2]$, the real part of the complex gap vanishes with the system size squared but grows exponentially with s and is given by the expression

$$\Gamma \approx \frac{2\pi^2}{N^2} e^{s/2 - s_{1/2}} \cosh\left(\frac{\sigma}{2}\right) \tag{40}$$

This estimate is tested in Fig.5. To obtain this expression we use the 2D electrostatics picture previously described. The density of states is $\rho(\epsilon) = N/\sigma\epsilon$, where $\epsilon \in [a,b]$ and $a = \epsilon_0$, $b = \exp[\sigma]\epsilon_0$. The electrostatic potential along the real axis equation (18), can be calculated analytically and is given by (see top panel of Fig.6)

$$V(\epsilon) = \ln(|\epsilon - b|)\ln\left(\frac{b}{\epsilon}\right) + \ln(|\epsilon - a|)\ln\left(\frac{\epsilon}{a}\right) + \tag{41}$$

$$+ \mathrm{Li}_2\left(1 - \frac{b}{\epsilon}\right) + \mathrm{Li}_2\left(1 - \frac{a}{\epsilon}\right) \tag{42}$$

However, to determine the real part of the complex gap it is enough to realise that the equipotential contour in the complex plane, $V(x,y) = V(0)$, is approximately a parabola near the origin (see Fig.6 for an illustration). Thus, expanding equation (16) to second order near the origin, we have

$$V(x,y) \approx C_0 - C_1 x + \frac{1}{2}C_2 y^2 \tag{43}$$

where the coefficients C_n are defined

$$C_n = \int_a^b \frac{1}{x^n}\rho(x)dx \tag{44}$$

Notice that $C_0 = V(0)$, $C_1 = E_x(x,0)$. Since we are interested in the contour $V(x,y) = V(0)$, we obtain

$$x = \frac{1}{2}\frac{C_2}{C_1}y^2 \tag{45}$$

For the given density of states we obtain

$$C \equiv \frac{1}{2}\frac{C_2}{C_1} = \frac{1}{2}e^{-s/2}\cosh\left(\frac{\sigma}{2}\right) \tag{46}$$

The gap is determined by integrating the electric field, $\vec{E}(x,y) = -\vec{\nabla}V$, along the parabola of equation (45)

$$\int_0^{\sqrt{\Gamma/C}} \left|\vec{E}(x,y)\right| dy = 2\pi \tag{47}$$

This is equivalent, through Cauchy Riemann, to the requirement $A(\Gamma,0) = 2\pi$. The integrand is approximated by $|\vec{E}(x,y)| \approx |\vec{E}(0,0)|$ by which we obtain an estimate for the gap

$$\Gamma \approx \frac{4\pi^2 C}{\left|\vec{E}(0,0)\right|^2} = \frac{2\pi^2}{N^2}e^{s/2 - s_{1/2}}\cosh\left(\frac{\sigma}{2}\right) \tag{48}$$

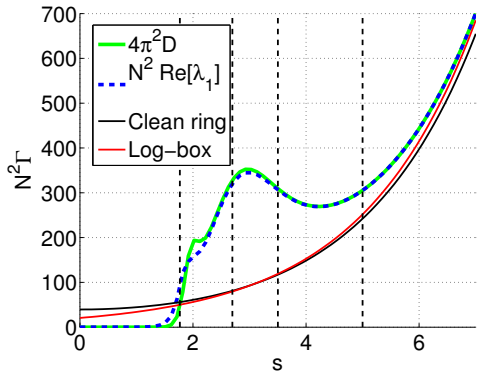

FIG. 5. The relaxation rate $\Gamma = \mathrm{Re}[\lambda_1]$ versus the affinity s for $N = 1000$ sites $\sigma = 5$. The non monotonic dashed blue line has been obtained via numerical diagonalization, whereas the solid green was obtained by calculating the diffusion coefficient as in [22]. The monotonic lines correspond to the limits of clean ring (equation (38), black) and $s > s_\infty$ (equation (40), red). The vertical dashed lines are the affinities s_μ that are associated with the scaled values $\mu = 1/2,\ 1,\ 2,\ \infty$ (from left to right).

IX. COMPLEXITY SATURATION FOR $s \gg s_\infty$

The secular equation for the eigenvalues is given by equation (15). In the nonconservative case, the eigenvalues of $\boldsymbol{H}$ do not depend on s, thus raising s will eventually make the entire spectrum complex. For a conservative matrix, however, $V(\epsilon)$ is also a function of s, so increasing s raises $V(\epsilon)$ at the same rate. Due to the conservative property, the eigenvalues of the associated hermitian martix, ϵ_j grow proportionaly to e^s. Increasing $s \to s + \Delta s$, we have

$$\sum_k \ln\left(\frac{z-\epsilon_k e^{\Delta s}}{\overline{w}}\right) = \ln\left[2\cosh\left(\frac{(s+\Delta s)N}{2}\right) - 2\right] \quad (49)$$

$$\sum_k \ln\left(\frac{z e^{-\Delta s}-\epsilon_k}{\overline{w}}\right) + N\Delta s = \ln\left[2\cosh\left(\frac{sN}{2}\right) - 2\right] + N\Delta s \quad (50)$$

but z is just a dummy variable, so we can redefine $z := z e^{-\Delta s}$ and the equation is unchanged. Thus increasing s does not change the number of complex solutions, as shown in Fig.7.

To estimate the the saturation value of the fraction of complex eigenvalues, we assume $s \gg s_\infty$. The eigenvalues have a log-box distribution so the potential along the real axis is

$$V(\epsilon) = \int_a^b \ln|\epsilon - \epsilon'|\rho(\epsilon')d\epsilon' = \quad (51)$$

$$= \frac{N}{2\sigma}\int_{-\sigma}^{\sigma} \ln\left|e^{(s+\mathscr{E}_c)/2} - e^{(s+\mathscr{E})/2}\right| d\mathscr{E} \quad (52)$$

Define $\mathscr{E}_c$ such that the eigenvalues with $\mathscr{E}$ in the range $-\sigma < \mathscr{E} < \mathscr{E}_c$ are complex, $\mathscr{E}_c$ is determined by the equation $V(\epsilon = e^{(s+\mathscr{E}_c)/2}) = V(0) = sN/2$, leading to

$$\int_{-\sigma}^{\sigma} \ln\left|e^{\mathscr{E}/2} - e^{\mathscr{E}_c/2}\right| d\mathscr{E} = 0 \quad (53)$$

Clearly, $\mathscr{E}_c$ depends only on σ (and not on N) (Fig.7). The fraction of complex eigenvalues is just

$$n = \frac{\int_a^{\epsilon_c}\frac{1}{\epsilon}d\epsilon}{\int_a^b \frac{1}{\epsilon}d\epsilon} = \frac{1}{\sigma}\ln\left(\frac{\epsilon_c}{a}\right) = \frac{\mathscr{E}_c + \sigma}{2\sigma} \quad (54)$$

The percolation transition is reflected in the complexity saturation. If $\alpha \lesssim 1$ there is saturation, but the crossover is not as sharp and the saturation value is lower than equation (54) and has a wider ensemble distribution. This is demonstrated in the bottom panel of Fig.7. The argument for complexity saturation stems from the fact that for $s \gg s_\infty$ the matrix $\boldsymbol{H}$ is diagonal and the eigenvalues are trivially localized. If $w_n = 1$ ($\alpha = \infty$), the eigenvalues are log-box distributed. In the resistor network limit ($\sigma = 0$ and finite α), the eigenvalues are again trivially localized, but with the exponent derived in section (VII A). This leads to a lower saturation value that can be calculated by the same method used to derive equation (54). In the general case where $\sigma \neq 0$ and $\alpha < \infty$, the calculation is more difficult, but it can be written formally as

$$\int \ln(\epsilon_c - \gamma) P(\gamma) d\gamma = 0 \quad (55)$$

where $\gamma = w e^{\mathscr{E}/2}$ and $P(\gamma)$ is the probability distribution. Generally, when $\alpha < \infty$ the couplings are no longer equal and can be very small, thus for small s, $\boldsymbol{H}$ is no longer trivially localized and the eigenvalues have some complicated distribution. Specifically, the limits of the integral depend on the realization of disorder, which explains the dispersion of the saturation value from sample to sample.

X. DISCUSSION

To summarize [14], they use a different method, bypassing the hermitization procedure. The long time behavior of v and D is deduced by numerical observations of the lower edge of the spectrum (small $|\lambda|$). In fact the hermitization procedure is claimed to obscure the complexity transition (we found it!). Somehow they do not bridge between complexity of the spectrum and the sliding transition in a purely conservative model. They make some comments regarding complexity and sliding in the following respect. They consider a model where there are two types of unit cells. Each unit cell is made of two bonds. The chain is composed of unit cells drawn from a bimodal distribution. Real eigenvalues only appear due to non conservative diagonal disorder (detachment rate). They do not find an explicit crossover to complexity and do not handle the purely conservative case.

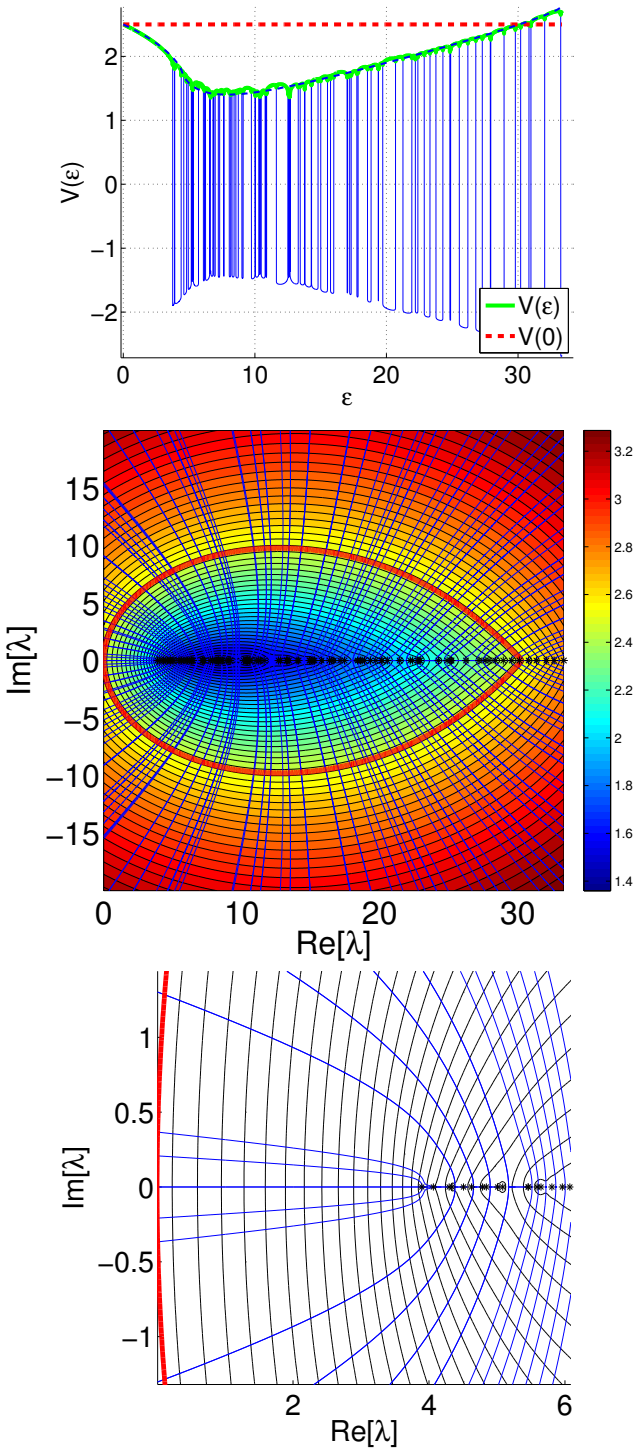

FIG. 6. **Top panel**: The electrostatic potential $V(\epsilon)$ along the real axis. The dashed blue line is the analytical result assuming $\rho = N(\sigma x)^{-1}$, equation (41). The stars indicate the position of the "charges", which are the eigenvalues of the associated Hermitian matrix, ε_j. **Middle panel**: The electrostatic potential $\Psi(z)$ of equation (16). Here we consider a ring with $N = 100$ sites, $\sigma = 2$ and $s = 5$. The complex λ_k spectrum is obtained by looking for the intersections of the field lineswith the red thick equipotential line $V(z) = V(0,0)$ that goes through the origin. **Bottom panel**: Zoom. Note that the complex spectrum unlike the real spectrum does not have a gap.

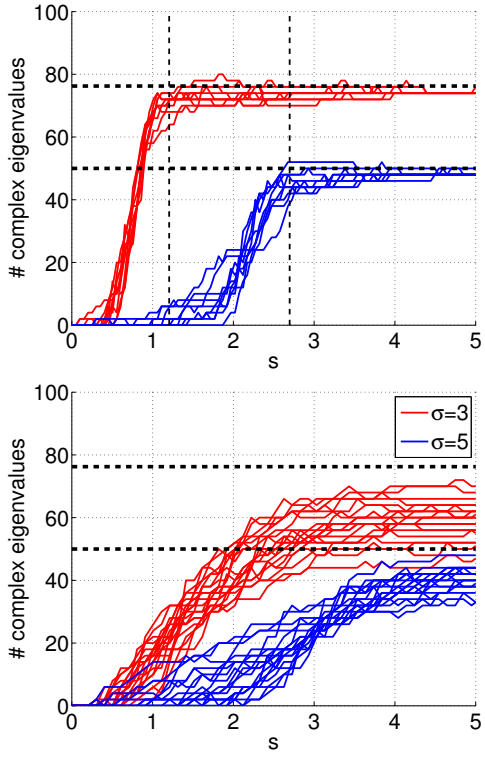

FIG. 7. We count the number of complex eigenvalues for a ring with $N = 100$ sites, for various values of the affinity s. Each red line corresponds to a different realization of field disorder with $\sigma = 3$ (red) and $\sigma = 5$ (blue). The black vertical lines are at values of $s_1(\sigma)$ at which the sliding transition occurs. We see that the asymptotic fraction of complex eigenvalues saturates, which is quite different from what is known for non-conservative non-Hermitian matrices. The horizontal dashed line are analytical estimates of equation (54). If the lattice were continuous and the disorder white noise, the number of complex eigenvalues would go from 0 to 100 at $s = s_{1/2}$. On the bottom panel $\alpha = 0.9$, the crossover is blurred and the saturation value is lower (the horizontal lines are calculated for $\alpha = \infty$).

[1] A. Amir, Y. Oreg, and Y. Imry, "On relaxations and aging of various glasses," *Proceedings of the National Academy of Sciences*, vol. 109, no. 6, pp. 1850–1855, 2012.
[2] A. Vaknin, Z. Ovadyahu, and M. Pollak, "Aging effects in an anderson insulator," *Phys. Rev. Lett.*, vol. 84, pp. 3402–3405, Apr 2000.
[3] A. Amir, Y. Oreg, and Y. Imry, "Slow relaxations and aging in the electron glass," *Phys. Rev. Lett.*, vol. 103, p. 126403, Sep 2009.
[4] Y. de Leeuw and D. Cohen, "Diffusion in sparse networks: Linear to semilinear crossover," *Phys. Rev. E*, vol. 86, p. 051120, Nov 2012.
[5] J.-P. Bouchaud and A. Georges, "Anomalous diffusion in disordered media: Statistical mechanisms, models and physical applications," *Physics Reports*, vol. 195, no. 45, pp. 127 – 293, 1990.
[6] Y. G. Sinai, "Limit behaviour of one-dimensional random walks in random environments," *Teoriya Veroyatnostei i ee Primeneniya*, vol. 27, no. 2, pp. 247–258, 1982.
[7] B. Derrida, "Velocity and diffusion constant of a periodic one-dimensional hopping model," *Journal of Statistical Physics*, vol. 31, no. 3, pp. 433–450, 1983.
[8] J. Bouchaud, A. Comtet, A. Georges, and P. L. Doussal, "Classical diffusion of a particle in a one-dimensional random force field," *Annals of Physics*, vol. 201, no. 2, pp. 285 – 341, 1990.
[9] D. K. Lubensky and D. R. Nelson, "Pulling pinned polymers and unzipping dna," *Phys. Rev. Lett.*, vol. 85, pp. 1572–1575, Aug 2000.
[10] D. K. Lubensky and D. R. Nelson, "Single molecule statistics and the polynucleotide unzipping transition," *Phys. Rev. E*, vol. 65, p. 031917, Mar 2002.
[11] D. R. Nelson and N. M. Shnerb, "Non-hermitian localization and population biology," *Phys. Rev. E*, vol. 58, pp. 1383–1403, Aug 1998.
[12] K. A. Dahmen, D. R. Nelson, and N. M. Shnerb, "Population dynamics and non-hermitian localization," in *Statistical mechanics of biocomplexity*, pp. 124–151, Springer, 1999.
[13] Y. Kafri, D. K. Lubensky, and D. R. Nelson, "Dynamics of molecular motors and polymer translocation with sequence heterogeneity," *Biophysical Journal*, vol. 86, no. 6, pp. 3373 – 3391, 2004.
[14] Y. Kafri, D. K. Lubensky, and D. R. Nelson, "Dynamics of molecular motors with finite processivity on heterogeneous tracks," *Phys. Rev. E*, vol. 71, p. 041906, Apr 2005.
[15] N. Hatano and D. R. Nelson, "Localization transitions in non-hermitian quantum mechanics," *Phys. Rev. Lett.*, vol. 77, pp. 570–573, Jul 1996.
[16] N. Hatano and D. R. Nelson, "Vortex pinning and non-hermitian quantum mechanics," *Phys. Rev. B*, vol. 56, pp. 8651–8673, Oct 1997.
[17] N. M. Shnerb and D. R. Nelson, "Winding numbers, complex currents, and non-hermitian localization," *Phys. Rev. Lett.*, vol. 80, pp. 5172–5175, Jun 1998.
[18] P. W. Brouwer, P. G. Silvestrov, and C. W. J. Beenakker, "Theory of directed localization in one dimension," *Phys. Rev. B*, vol. 56, pp. R4333–R4335, Aug 1997.
[19] I. Y. Goldsheid and B. A. Khoruzhenko, "Distribution of eigenvalues in non-hermitian anderson models," *Phys. Rev. Lett.*, vol. 80, pp. 2897–2900, Mar 1998.
[20] J. Feinberg and A. Zee, "Non-hermitian localization and delocalization," *Phys. Rev. E*, vol. 59, pp. 6433–6443, Jun 1999.
[21] S. Alexander, J. Bernasconi, W. R. Schneider, and R. Orbach, "Excitation dynamics in random one-dimensional systems," *Rev. Mod. Phys.*, vol. 53, pp. 175–198, Apr 1981.
[22] D. Hurowitz and D. Cohen, "Nonequilibrium version of the einstein relation," *Phys. Rev. E*, vol. 90, p. 032129, Sep 2014.
[23] L. G. Molinari, "Determinants of block tridiagonal matrices," *Linear Algebra and its Applications*, vol. 429, no. 89, pp. 2221 – 2226, 2008.

ACKNOWLEDGEMENTS

This research has been supported by by the Israel Science Foundation (grant No. 29/11).

Appendix A: Finding the sign of $V'(0)$

To derive equation (21) we assume an integrated density of states corresponding to equation (3), $\mathcal{N}(\epsilon) = (\epsilon/\epsilon_c)^{\mu}$, where ϵ_c is some cutoff due to the discreteness of the lattice. The electrostatic potential along the real axis is given by (integration by parts of equation (18))

$$V(\epsilon) = -\int_0^{\epsilon_c} \frac{\mathcal{N}(x)}{x-\epsilon} dx \tag{A1}$$

and the derivative with respect to ϵ at the origin is (after integrating by parts)

$$\begin{aligned} V'(\epsilon) &= \int_0^{\epsilon_c} \frac{\rho(x)}{x-\epsilon} dx = && \text{(A2)} \\ &= \frac{\mu}{\epsilon_c^{\mu}} \int_0^{\epsilon_c} \frac{x^{\mu-1}}{x-\epsilon} dx \; = && \text{(A3)} \\ &= \frac{\mu}{\epsilon_c^{\mu}} \epsilon^{\mu-1} \int_0^{z_c} \frac{z^{\mu-1}}{z-1} dz = \frac{\mu}{\epsilon_c^{\mu}} \epsilon^{\mu-1} I(\epsilon) = \rho(\epsilon) I(\epsilon) && \text{(A4)} \end{aligned}$$

where we substituted $z = x/\epsilon$ and defined

$$I(\epsilon) = \int_0^{z_c} \frac{z^{\mu-1}}{z-1} dz \,, \quad z_c = \frac{\epsilon_c}{\epsilon} \tag{A5}$$

The integral converges for $\mu < 1$. The integral can be written in terms of Incomplete Euler Beta functions defined as

$$B_u(a,b) = \int_0^u x^{a-1}(1-x)^{b-1} dx \tag{A6}$$

However one must be careful and take only the Cauchy principal part

$$\begin{aligned} \lim_{\epsilon\to 0} I &= \lim_{\epsilon\to 0} \int_0^{z_c} \frac{z^{\mu-1}}{z-1} dz = && \text{(A7)} \\ &= \lim_{\epsilon\to 0} \lim_{\delta\to 0} \left[\int_0^{1-\delta} x^{\mu-1}(1-z)^{-1} dz + \int_{1+\delta}^{z_c} z^{\mu-1}(1-z)^{-1} dz \right] = && \text{(A8)} \\ &= \lim_{\epsilon\to 0} \lim_{\delta\to 0} \left[B_{1-\delta}(\mu,0) + \int_{1+\delta}^{z_c} z^{\mu-1}(1-z)^{-1} dz \right] && \text{(A9)} \\ &= \lim_{\epsilon\to 0} \lim_{\delta\to 0} \left[B_{1-\delta}(\mu,0) - \int_{1/z_c}^{1-\delta} t^{-\mu}(1-t)^{-1} dx \right] && \text{(A10)} \\ &= \lim_{\delta\to 0} [B_{1-\delta}(\mu,0) - B_{1-\delta}(1-\mu,0)] = && \text{(A11)} \\ &= \psi(1-\mu) - \psi(\mu) = \pi \cot(\pi\mu) && \text{(A12)} \end{aligned}$$

where $\psi(z)$ is the digamma function and the last equality was obtained by the reflection formula. To go from the fourth to the fifth line we took the limit $z_c =\!\!\rightarrow \infty$, which corresponds to $\epsilon \to 0$. It is clear that C and thus $V'(0^+)$ changes sign from positive to negative at $\mu = 1/2$.

Appendix B: Sliding transition - the definition of s_μ

In order to understand the dependence of v and D on N and s, it is useful to recall known results that have been obtained for the time-dependent spreading in an $N = \infty$ lattice. Recall that the drift is induced by the stochastic field, equation (6) whose affinity is defined

$$s = \frac{1}{N} \sum_{n=1}^{N} \mathscr{E}_{n\rightsquigarrow n+1} \tag{B1}$$

The cummulant generating function of the stochastic field can be written as $g(\mu) = (s - s_\mu)\mu$, where s_μ is defined via the following expression:

$$\left\langle e^{-\mathscr{E}\mu} \right\rangle \equiv \mathrm{e}^{-(s-s_\mu)\mu} \tag{B2}$$

If the stochastic field has normal distribution with standard deviation σ, then $s_\mu = (1/2)\sigma^2\mu$. For our box distribution with $\mathscr{E} \in [s-\sigma, s+\sigma]$,

$$s_\mu = \frac{1}{\mu}\ln\left(\frac{\sinh(\mu\sigma)}{\mu\sigma}\right) \tag{B3}$$

which is monotonically ascending from zero to $s_\infty = \sigma$. The positive monotonic function s_μ can be inverted, hence we can define a scaled affinity $\mu(s)$. Note that equation (B2) implies that $\mu(s)$ is the value of μ for which the left-hand-side equals unity.

It has been shown in [7] that the velocity (first moment) exhibits a transition at s_1 from zero to finite veloct. The diffusion (second moment) at s_2 goes from finite to divergent. In the text we showed that the delocalization transition occurs at $s_{1/2}$, which also corresponds to the diffusion coefficient going from sub-ohmic to super-ohmic [22].

Appendix C: The similarity transformation (definition of H)

The associated hermitian matrix $\boldsymbol{H}$ is obtained by a similarity transformation to a basis in which the stochastic field is uniform $\epsilon = s$, followed by setting $s = 0$ on the off diagonals.

$$\boldsymbol{W} = \begin{pmatrix} -\gamma_1 & w_1 e^{\mathscr{E}_1/2} & & w_N e^{-\mathscr{E}_N/2} \\ w_1 e^{-\mathscr{E}_1/2} & \ddots & \ddots & \\ & \ddots & \ddots & w_{N-1}e^{\mathscr{E}_{N-1}/2} \\ w_n e^{\mathscr{E}_N/2} & & w_{N-1}e^{-\mathscr{E}_{N-1}/2} & -\gamma_N \end{pmatrix} \tag{C1}$$

where the decay rates are determined by conservativity

$$\gamma_n = w_{n-1}e^{-\mathscr{E}_{n-1}/2} + w_n e^{\mathscr{E}_n/2} \tag{C2}$$

The following similarity transformation

$$U_{ij} = \delta_{ij}\exp\left[-\frac{1}{2}\sum_{k=1}^{j-1}\mathscr{E}_k + \frac{j-1}{2}\bar{s}\right], \tag{C3}$$

$$\bar{s} = \frac{1}{N}\sum_{k=1}^{N}\mathscr{E}_k \tag{C4}$$

reduces the rate equation to

$$\tilde{W} = U^{-1}WU = \begin{pmatrix} -\gamma_1 & w_1 e^{\bar{s}/2} & & w_N e^{-\bar{s}/2} \\ w_1 e^{-\bar{s}/2} & \ddots & \ddots & \\ & \ddots & \ddots & w_{N-1}e^{\bar{s}/2} \\ w_n e^{\bar{s}/2} & & -w_{N-1}e^{-\bar{s}/2} & -\gamma_N \end{pmatrix} \tag{C5}$$

The associated hermitian matrix is defined by setting $\bar{s} = 0$,

$$\boldsymbol{H} = \begin{pmatrix} -\gamma_1 & w_1 & & w_N \\ w_1 & \ddots & \ddots & \\ & \ddots & \ddots & w_{N-1} \\ w_n & & -w_{N-1} & -\gamma_N \end{pmatrix} \tag{C6}$$

which is of course real, symmetric and has real eigenvalues ϵ_k.

Appendix D: The formula for the spectral determinant

For the purpose of this section it makes things easier to define $\boldsymbol{\Gamma} = -\boldsymbol{W}$, the goal is to derive an expression for the spectral determinant

$$\det(\boldsymbol{\Gamma} - \lambda\boldsymbol{I}) = 0 \tag{D1}$$

in terms of the hermitian eigenvalues ϵ_k. This determinant can be calculated using a formula due to Molinari [23] for tridiagonal matrices. We define the matrix

$$T_n = \begin{pmatrix} \gamma_n - \lambda & -w_{n-1}^2 \\ 1 & 0 \end{pmatrix} \tag{D2}$$

The key point is that the matrices T_n are the same for $\mathbf{\Gamma}$ and for $\boldsymbol{H}$. Using the formula for the deteminant for both matrices, we obtain

$$\det(\boldsymbol{H} - \lambda \boldsymbol{I}) = \mathrm{tr}\left[\prod_{n=1}^{N} T_n\right] - 2\left[\prod_{n=1}^{N} w_n\right] \tag{D3}$$

$$\det(\mathbf{\Gamma} - \lambda \boldsymbol{I}) = \mathrm{tr}\left[\prod_{n=1}^{N} T_n\right] - 2\left[\prod_{n=1}^{N} w_n\right] \cosh\left(\frac{N\bar{s}}{2}\right) \tag{D4}$$

$$\tag{D5}$$

subtracting the equations and writing the characteristic polynomial of the Hermitian matrix

$$\det(\boldsymbol{H} - \lambda \boldsymbol{I}) \;=\; \prod_{n=1}^{N} (\epsilon_n - \lambda) \tag{D6}$$

we obtain an equation for the eigenvalues λ (equation (12))

$$\prod_{n=1}^{N} (\lambda - \epsilon_n) \;=\; \left[\prod_{n=1}^{N} w_n\right] 2\left(\cosh\left(\frac{N\bar{s}}{2}\right) - 1\right) \tag{D7}$$

According to Thouless, for the corresponding Hermitian problem

$$e^{N/\xi} = \prod_{n=1}^{N} \left(\frac{\epsilon - \epsilon_n}{w_n}\right) \tag{D8}$$

where $\xi(\epsilon)$ is the energy dependent localization length.

Appendix E: Clean ring

The real spectrum of a clean ring is doubly degenerate. The spectrum is completely complex. The potential oscillates and does not reach the "cosh line" and appears to have $N/2$ maxima. Introducing a small perturbation to one of the bonds, say $g = 1 - \varepsilon$ removes the degeneracy and raises the remaining maxima from $-\infty$.

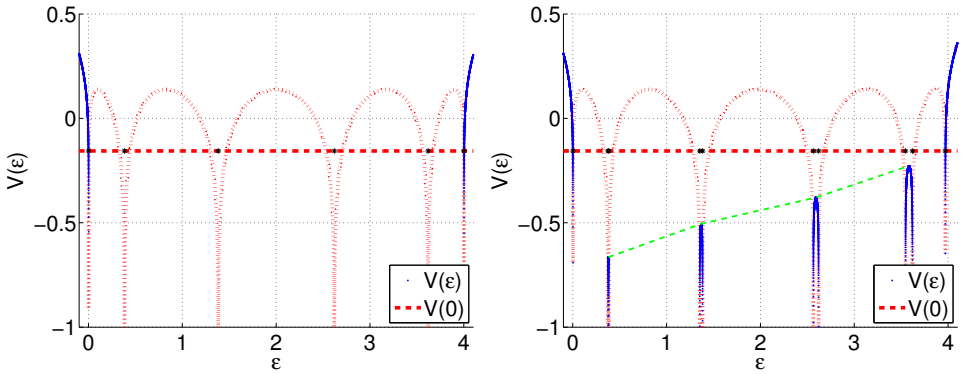

FIG. 8. Solving the secular equation for a clean ring. The left panel shows the electrostatic potential of a clean ring, which is double degenerate. In the right panel one of the bonds is perturbed. Here $N = 10$ and $g = 0.9$ and $s = 0.1$

Appendix F: Continuous ring

The purpose of this appendix is to derive the secular equations for the continuous version of a weak link and a stochastic field defect. The derivation is based on the transfer matrix method applied to the diffusion equation. We first present the transfer matrix method applied to the diffusion equation. In the following sections we introduce the matching conditions for piecewise constant $D(x)$ and $u(x)$ which are used to construct a weak link and a stochastic field defect.

The dynamics of the continuous limit is described by a diffusion equation with spatially dependent diffusion coefficient $D(x)$ and drift velocity $u(x)$

$$\frac{\partial \psi}{\partial t} = \frac{\partial}{\partial x}\left[D(x)\frac{\partial \psi}{\partial x} - u(x)\psi\right] = \frac{\partial}{\partial x}\left[D(x)\frac{\partial \psi}{\partial x}\right] - \frac{\partial}{\partial x}\left[u(x)\psi\right] \tag{F1}$$

Assuming that $D(x)$ and $u(x)$ are piecewise constant, the solution to the diffusion equation in each region is simply $\psi \sim e^{-\lambda t + ikx}$, inserting this in equation (F1), we obtain the dispersion relation

$$\lambda = Dk^2 + iuk = D\left(k + \frac{iu}{2D}\right)^2 + \frac{u^2}{4D} \tag{F2}$$

$$k_\pm = \frac{-iu \pm \sqrt{4\lambda D - u^2}}{2D} = \frac{-is}{2} \pm \sqrt{\frac{\lambda}{D} - \frac{s^2}{4}} \tag{F3}$$

$$\equiv \frac{-is}{2} \pm \tilde{k} \tag{F4}$$

So, in each region the solution to equation (F1) is a superposition of clock wise (k_+) and counterclockwise (k_-) waves

$$\psi(x) = Ae^{ik_+x} + Be^{ik_-x} = \tag{F5}$$

$$= \mathrm{e}^{\frac{u}{2D}x}\left(Ae^{i\frac{\sqrt{4\lambda D - u^2}}{2D}x} + Be^{-i\frac{\sqrt{4\lambda D - u^2}}{2D}x}\right) = \tag{F6}$$

$$= \psi^+(x) + \psi^-(x) \tag{F7}$$

From now on we replace $\tilde{k} \to k$. We define the vector

$$\begin{pmatrix} \psi^+(x) \\ \psi^-(x) \end{pmatrix} \tag{F8}$$

In the next section it will be more convenient to work with the vector

$$\begin{pmatrix} \psi \\ \partial\psi \end{pmatrix} = \begin{pmatrix} 1 & 1 \\ ik_+ & ik_- \end{pmatrix}\begin{pmatrix} \psi^+(x) \\ \psi^-(x) \end{pmatrix} \tag{F9}$$

The transfer matrix is along a distance x is $UT(x)U^{-1}$ where

$$U = \begin{pmatrix} 1 & 1 \\ ik + \frac{is}{2} & -ik + \frac{is}{2} \end{pmatrix} \tag{F10}$$

and

$$T = \begin{pmatrix} e^{i\left(k - \frac{is}{2}\right)x} & 0 \\ 0 & e^{i\left(-k - \frac{is}{2}\right)x} \end{pmatrix} \tag{F11}$$

such that for a segment of length L

$$\left.\begin{pmatrix} \psi \\ \partial\psi \end{pmatrix}\right|_{x=0} = UT(L)U^{-1}\left.\begin{pmatrix} \psi \\ \partial\psi \end{pmatrix}\right|_{x=L} \tag{F12}$$

Appendix G: Ring with weak link "g"

The purpose of this section is to derive equation (31), which is the condition for complexity in a ring with a weak link, in the continuum limit. The ring has circumference L and a weak link, which is a small region $|x| < a/2$ where the diffusion coefficient is much lower than the rest of the ring. We define

$$D(x) = \begin{cases} D_0, & |x| < a/2 \\ D, & |x| > a/2 \end{cases} \tag{G1}$$

To make life simple we define dimensionless variables. The strength of the scatterrer

$$g \equiv \frac{L}{a} \cdot \frac{D_0}{D} \tag{G2}$$

where g is constant in the limit $a \to 0,\ D_0 \to 0$. For the diffusion equation to be continuous we demand continuity of the wave function ψ and of the current $J = D(x)\partial\psi - u(x)\psi$ in all of space. Specifically, this must hold at the points $x = \pm a/2$. In matrix form, this requirement can be written as

$$\left(\begin{array}{c} \psi \\ \partial\psi \end{array} \right)\Big|_{\pm\frac{1}{2}a^-} = \left(\begin{array}{cc} 1 & 0 \\ 0 & \left(\frac{D}{D_0}\right)^{\pm 1} \end{array} \right) \left(\begin{array}{c} \psi \\ \partial\psi \end{array} \right)\Big|_{\pm\frac{1}{2}a^+} \tag{G3}$$

thus we define the matrix

$$S = \left(\begin{array}{cc} 1 & 0 \\ 0 & \frac{D}{D_0} \end{array} \right) \tag{G4}$$

constructing the path across the barrier, we write

$$\vec{\psi}(-a/2) = S^{-1}UT(a)U^{-1}S\vec{\psi}(a/2) \tag{G5}$$

Taking the limit $a \to 0$ and $D_0 \to 0$ we obtain the matching requirement across a weak link

$$M = \lim_{a,D_0\to 0} S^{-1}UT(a)U^{-1}S = \left(\begin{array}{cc} 1 & L/g \\ 0 & 1 \end{array} \right) \tag{G6}$$

Note that we set $s = 0$ within the segment $|x| < a/2$, this is ok since we took the limit $a \to 0$ later on.

To obtain the secular equation, we simply construct the path along the entire ring and apply periodic boundary conditions

$$\vec{\psi}(0) = UT(L/2)U^{-1}MUT(L/2)U^{-1}\vec{\psi}(0) \tag{G7}$$

this equation has a non trivial solution provided that

$$\det\left(T(L/2)U^{-1}MUT(L/2) - I\right) = 0 \tag{G8}$$

restoring the notation of $\tilde{k}$, this equation reduces to

$$\cos(\tilde{k}L) + \frac{L}{g}\frac{\tilde{k}^2 + s^2/4}{2\tilde{k}}\sin(\tilde{k}L) = \cosh(sL/2) \tag{G9}$$

where

$$\tilde{k} = \sqrt{\frac{\lambda}{D} - \frac{s^2}{4}} \tag{G10}$$

defining dimensionless momentum $q = \tilde{k}L$ and total affinity $S = sL$, the secular equation is

$$\cos(q) + \frac{1}{g}\frac{q^2 + S^2/4}{2q}\sin(q) = \cosh(S/2) \tag{G11}$$

The left hand side is an oscillating function within an envelope

$$A(q) = \sqrt{1 + \frac{1}{g^2}\left(\frac{q^2 + S^2/4}{2q}\right)^2} \tag{G12}$$

which has a minimum at $q_{min} = S/2$, so complex solutions are possible provided $A(q_{min}) > \cosh(S/2)$, which yields an equation for the value of S necessary for complex eigenvalues to appear.

$$\sqrt{1 + \left(\frac{S}{2g}\right)^2} > \cosh\left(\frac{S}{2}\right) \tag{G13}$$

1. Ground state of associated hermitian problem, ϵ_1

The eigenvalues of the associated hermitian problem are (in analogy with the definition of $\boldsymbol{H}$)

$$\epsilon_k = D\left(k^2 + \frac{s^2}{4}\right) \tag{G14}$$

and k is determined by the secular equation equation (G11) with $s = 0$ on the right hand side. This leads to the equation

$$\cos(q_\epsilon) + \frac{1}{g}\frac{q_\epsilon^2 + (\frac{S}{2})^2}{2q_\epsilon}\sin(q_\epsilon) = 1 \tag{G15}$$

where we have defined $q_\epsilon = kL$ according to equation (G14). If $S = 0$, then $\epsilon_k = \lambda_k$, so when S is small we expect some correction. Thus, we expand equation (G15) around $q_\epsilon = iS/2$ which corresponds to $\lambda = 0$, expand in powers of S and solve for q_{ϵ_0} to obtain

$$q_{\epsilon_0}^2 = \frac{S^2}{4}\frac{1}{g-1} \tag{G16}$$

and from equation (G14)

$$\epsilon_1 = \frac{S^2}{4}\frac{g}{g-1} \tag{G17}$$

Appendix H: Ring with single field defect

The field defect of the discrete ring translates to a defect in the velocity field in the continuum limit. We define a region $|x| < a/2$ in which the velocity field is different. For $|x| > a$ we have $u/D = s$ and for $|x| < a$ we have $u/D = s + \sigma$. Note that for there to be a transition from real to complex s and σ must have opposite signs. The boundary conditions are that the wave function and the current be continuous everywhere. Applying the boundary conditions across the defect and taking the limit $a \to 0$ such that $a\sigma = \Sigma(\text{const})$ we obtain the matching matrix at each boundary of the defect

$$S = \begin{pmatrix} 1 & 0 \\ \sigma & 1 \end{pmatrix} \tag{H1}$$

where S is at $x = a/2$ and S^{-1} at $x = -a/2$. The transfer matrix is along a distance x is $UT(x)U^{-1}$ where

$$U = \begin{pmatrix} 1 & 1 \\ i\tilde{k}_\sigma + \frac{is}{2} & -i\tilde{k}_\sigma + \frac{is}{2} \end{pmatrix} \tag{H2}$$

and

$$T = \begin{pmatrix} e^{i(\tilde{k}_\sigma - \frac{is}{2})x} & 0 \\ 0 & e^{i(-\tilde{k}_\sigma - \frac{is}{2})x} \end{pmatrix} \tag{H3}$$

Note that inside the defect $s \to s + \sigma$ and $\tilde{k} \to \tilde{k}_\sigma = \sqrt{\lambda/D - (s+\sigma)^2/4}$ while outside the defect $s \to s$ and $\tilde{k} \to \sqrt{\lambda/D - s^2/4}$. The matching condition between two sides of the defect is obtained by propagating the wave between the edges of the defect and taking the limit $a \to 0$ while keeping $a\sigma$ constant,

$$M = \lim_{a\to 0} S^{-1}U_\sigma T_\sigma(a)U_\sigma^{-1}S = \begin{pmatrix} e^\Sigma & 0 \\ (-1+e^\Sigma)s & 1 \end{pmatrix} \tag{H4}$$

The subscript σ is to indicate that $\sigma \neq 0$/ For a ring the wave function must obey

$$\begin{pmatrix} \psi \\ \partial\psi \end{pmatrix}\Big|_{x=0} = T(L/2)MT(L/2)\begin{pmatrix} \psi \\ \partial\psi \end{pmatrix}\Big|_{x=0} \tag{H5}$$

which is possible only if

$$|T(L/2)MT(L/2) - I| = 0 \tag{H6}$$

This is the secular equation, which takes the explicit form

$$\cos\left(\frac{1}{2}\sqrt{4\lambda-S^2}\right)\cosh\left(\frac{\Sigma}{2}\right)+\frac{\sin\left(\frac{1}{2}\sqrt{4\lambda-S^2}\right)}{\sqrt{4\lambda-S^2}}S\sinh\left(\frac{\Sigma}{2}\right)=\cosh\left(\frac{S+\Sigma}{2}\right) \tag{H7}$$

It is easy to verify that $\lambda=0$ is a solution as required. The envelope function is

$$A(\lambda)=\sqrt{\cosh^2\left(\frac{\Sigma}{2}\right)+\frac{S^2}{4\lambda-S^2}\sinh^2\left(\frac{\Sigma}{2}\right)} \tag{H8}$$

with $A(0)=\cosh\left((S+\Sigma)/2\right)$. The envelope function is monotonically decreasing for $\lambda>S^2/4$ reaching an asymptotic value

$$\lim_{\lambda\to\infty}A(\lambda)=\cosh\left(\frac{\Sigma}{2}\right) \tag{H9}$$

Note that the true envelope function does not really explode at $\lambda=S^2/4$, because $\sinh(x)/x\to 1$ as $x\to 0$. The condition for complexity is that

$$A(0)>A(\infty) \tag{H10}$$

So S_c is defined by the equation

$$\cosh\left(\frac{S+\Sigma}{2}\right)=\cosh\left(\frac{\Sigma}{2}\right) \tag{H11}$$

As defined in the text, the affinity is the mean of the stochastic field, $s=(S+\Sigma)/L$, thus the equation has a solution at $sL=\Sigma$

$$s_cL=\sigma a\ \ \Rightarrow\ \ s_c=\frac{\sigma}{N} \tag{H12}$$

as in equation (26) of the text.

Appendix I: Ring with white disorder (French)

The density of states and electrostatic potential can be obtained analytically for a one dimensional diffusion problem with a stochastic force field that is gaussian white noise with variance $\mathrm{Var}(\mathscr{E})=\sigma/a^2$ [8]. All of the couplings are the same, $D_0=a^2w\equiv 1$. We summarize these results here in our notations.

$$z\equiv 16\frac{D_0^3}{\sigma^2}\epsilon \tag{I1}$$

So the integrated density of states is

$$\mathscr{N}(z)=\frac{\sigma N}{2D_0^2\pi^2}\frac{1}{M_\mu^2(\sqrt{z})} \tag{I2}$$

Note that in the limit $\epsilon\to\infty$ the free particle result is recovered $\mathscr{N}(\epsilon)=\frac{N}{\pi}\sqrt{\epsilon}$. The electrostatic potential is

$$V(z)=-\sqrt{z}\frac{M'_\mu(\sqrt{z})}{M_\mu(\sqrt{z})}\frac{\sigma}{4D_0^2},\ \ z\geq 0 \tag{I3}$$

where

$$M_\mu(z)=\sqrt{J(z)_\mu^2+Y(z)_\mu^2} \tag{I4}$$

and J_μ and Y_μ are Bessel functions of the first and second kind. In the limit $\epsilon\to 0$ we have for $\mu>0$

$$V(\epsilon)=\begin{cases}\mu\nearrow 1/2, & \mu<1/2\\ \mu\searrow 1/2, & \mu>1/2\end{cases} \tag{I5}$$

Appendix J: Step by step electrostatics

The building blocks of the analysis are an isolated state, or point charge and a continuum Fig.9. From these blocks we can construct any relevant 2D electrostatic potential.

Point charge. The potential of a single charge is simply

$$V_{\text{charge}}(R) = \ln|R-\epsilon_1| \tag{J1}$$

Uniform charge. For a uniform charge distribution on the interval $x \in [a,b]$, the potential is given by the integral

$$V(R) = \frac{1}{b-a}\int_a^b \ln|R-x|dx = \tag{J2}$$

$$= \frac{1}{b-a}\left[(R-a)\ln|R-a| - (R-b)\ln|R-b| + a - b\right] \tag{J3}$$

which has a minimum at $R = (a+b)/2$ and resembles a "soft well" potential.

Continuum (clean ring).

For a continuum, or clean ring we show that the density is higher at the edges, leading to a "flat floor" potential.

The associated hermitian spectrum of a clean lattice ring is obtained by appropriately setting $s = 0$ in equation(37)

$$\epsilon_n = 2w\left[\cosh\left(\frac{s}{2}\right) - \cos\left(\frac{2\pi}{N}n\right)\right] \tag{J4}$$

which can be inverted to obtain the integrated density of states

$$\mathcal{N}(\epsilon) = \frac{N}{2\pi}\arccos\left[\cosh\left(\frac{s}{2}\right) - \frac{\epsilon}{2w}\right] \tag{J5}$$

The density of states is

$$\rho(\epsilon) = \frac{d\mathcal{N}}{d\epsilon} = \frac{N}{4\pi w}\left[1 - \left(\cosh\left(\frac{s}{2}\right) - \frac{\epsilon}{2w}\right)^2\right]^{-1/2} \tag{J6}$$

from which we obtain

$$\rho(k) = \frac{N}{4\pi w}\left[1-\cos^2(k)\right]^{-1/2} = \frac{N}{4\pi w\sin(k)} \tag{J7}$$

The electrostatic potential formed by a charge distribution $\rho(\epsilon)$ is given by means of equation(18)

$$V(R) = \int_a^b \ln\left|\frac{\epsilon - R}{w}\right|\rho(\epsilon)d\epsilon = \frac{N}{2\pi}\int_0^{2\pi}\ln\left|2\cosh\left(\frac{s}{2}\right) - 2\cos(k) - R\right|dk \tag{J8}$$

where $[a,b] = 2w[\cosh(s/2)\pm 1]$.

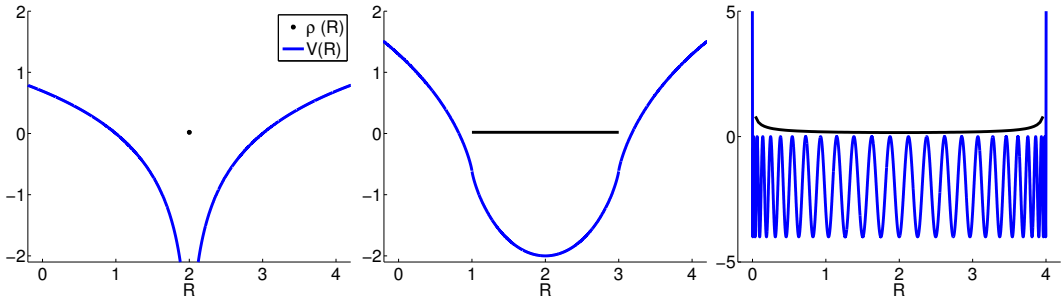

FIG. 9. The building blocks of the electrostatic picture. A point charge at $R = 2$ (left) generates a logarithmic potential, a uniform charge distribution on the interval $[1,3]$ (middle) generates a soft well and a clean ring with $s = 0$ (right) generates a flat floor (any $s \neq 0$ just shifts the charge density to the right). The potential is the blue line and the charge density is drawn in black. For the clean ring we plot the spectral determinant instead of the potential, in order to show that the floor is really at zero.